iScience

CellPress
OPEN ACCESS

Article

Social modulation of individual preferences in cockroaches

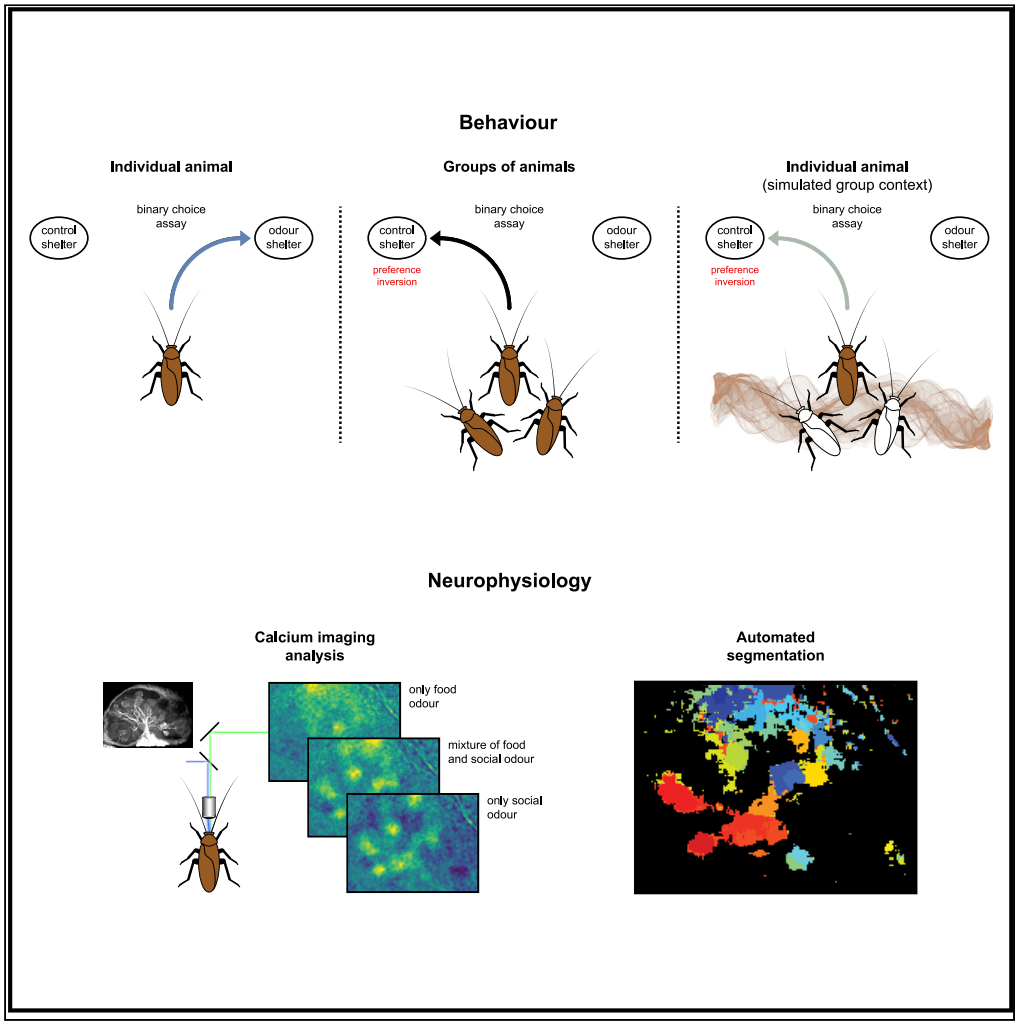

Yannick Günzel, Jaclyn McCollum, Marco Paoli, C. Giovanni Galizia, Inga Petelski, Einat Couzin-Fuchs

einat.couzin@uni-konstanz.de

HIGHLIGHTS

Cockroaches invert their innate preference to vanillin when in a group

The inversion occurs also when the social context is replaced with a colony odor

Vanillin-related antennal lobe activity is reduced in presence of a colony odor

This could serve as a mechanism to avoid recently exploited resources

Günzel et al., iScience 24, 101964
January 22, 2021
https://doi.org/10.1016/j.isci.2020.101964

iScience

CellPress
OPEN ACCESS

Article

Social modulation of individual preferences in cockroaches

Yannick Günzel,[1,2,3,5] Jaclyn McCollum,[1,5] Marco Paoli,[1,4] C. Giovanni Galizia,[1,2] Inga Petelski,[1,3] and Einat Couzin-Fuchs[1,2,3,6,*]

Summary

In social species, decision-making is both influenced by, and in turn influences, the social context. This reciprocal feedback introduces coupling across scales, from the neural basis of sensing, to individual and collective decision-making. Here, we adopt an integrative approach investigating decision-making in dynamical social contexts. When choosing shelters, isolated cockroaches prefer vanillin-scented (food-associated) shelters over unscented ones, yet in groups, this preference is inverted. We demonstrate that this inversion can be replicated by replacing the full social context with social odors: presented alone food and social odors are attractive, yet when presented as a mixture they are avoided. Via antennal lobe calcium imaging, we show that neural activity in vanillin-responsive regions reduces as social odor concentration increases. Thus, we suggest that the mixture is evaluated as a distinct olfactory object with opposite valence, providing a mechanism that would naturally result in individuals avoiding what they perceive as recently exploited resources.

Introduction

Dissecting social feedbacks in collective behavior is notoriously difficult. While modeling has proven to be extremely valuable in constructing plausible hypotheses for how individual behavior scales to collective phenomena, alternative individual-level mechanisms may produce similar higher-order (*e.g.* group-level and population-level) patterns. In order to discriminate among alternative hypotheses—and also to allow the generation of new hypotheses—approaches that allow the tracking of individuals as they make decisions within their social context, as well as investigating the neural activity during decision-making, may prove to be invaluable. A common feature of decision-making in social species is that relevant information may be individually acquired or socially derived, and the key to achieve effective foraging is a context-dependent balance of both (Dunlap et al., 2016; Kendal and Collen, 2011; King and Cowlishaw, 2007; Miller et al., 2013; Rieucau and Giraldeau, 2011). Furthermore, the question whether to use social information, and to what degree, will often depend on the context (Dunlap et al., 2016; Kendal and Collen, 2011); for example, the presence of conspecifics on a resource patch may imply high food quality but also strong competition. In general, social information becomes more valuable when environmental cues are weak, unreliable, or costly to acquire (Ame et al., 2004; Dunlap et al., 2016; Kendal et al., 2004; Miller et al., 2013). Without an explicit calculation of reliability (Torney et al., 2009), inferring the preferences of conspecifics can provide a valuable indication of resource quality. At the same time, this information means that the resource has already been, at least partially, exploited (Canonge et al., 2011; Hall and Kramer, 2008).

How do animals balance individual and social information? The tractability of cockroaches for the study of collective behavior, and their easily accessible nervous system offer new opportunities to tackle this question (Amé et al., 2006; Lihoreau et al., 2012; Lihoreau and Rivault, 2011). Cockroaches reside in large and cohesive aggregates in dark shelters during their resting phase, which they leave mainly solitarily to locate resources in their home range (Durier and Rivault, 2000; Lihoreau et al., 2012). Different physical properties influence the decisions to settle in or to leave a shelter, including illumination level, humidity, and cues for food presence (Canonge et al., 2009; Doi and Toh, 1992; Martín et al., 2019). In addition, past visits, as well as presence of conspecifics, increase the probability of individuals to utilize a shelter, as long as it is not overcrowded (Ame et al., 2004; Canonge et al, 2009, 2011; Jeanson et al., 2005; Planas-Sitja et al., 2015). Taken together, these findings suggest that cockroach's shelter-selection behavior results from the

[1]Department of Biology, University of Konstanz, 78457 Konstanz, Germany

[2]Centre for the Advanced Study of Collective Behaviour, University of Konstanz, 78464 Konstanz, Germany

[3]Department of Collective Behaviour, Max Planck Institute of Animal Behavior, 78464 Konstanz, Germany

[4]CNRS, Research Centre for Animal Cognition, 31062 Toulouse Cedex 9, France

[5]These authors contributed equally

[6]Lead contact

*Correspondence: einat.couzin@uni-konstanz.de

https://doi.org/10.1016/j.isci.2020.101964

interplay between the tendency to aggregate and competition for resources, offering a model system to study the mechanisms underlying collective decision-making (Amé et al., 2006; Canonge et al., 2011).

Recently, it has been reported that individual cockroaches *Periplaneta americana* prefer vanillin-scented shelters over unscented controls in a binary choice assay (Laurent Salazar et al., 2017). Vanillin is known to be an attractant to cockroaches, most likely indicating a potential food source, as it can be found in various plants and decaying wood (Meyer and Norris, 1967). The preference for vanillin is reversed, however, when individuals are tested in a group (Laurent Salazar et al., 2017). Supported by a computational model, it has been suggested that this preference inversion can be accounted for if individuals exhibit a weaker social interaction in the presence of vanillin (Laurent Salazar et al., 2017; Martín et al., 2019). As a result, a stronger social amplification would occur in the absence of vanillin such that groups form more easily in the unscented shelter. A similar inversion phenomenon has also been observed when cockroaches were faced with shelters of different humidity levels: individuals showed the tendency to prefer humid shelters, while groups aggregate more in a drier alternative (Martín et al., 2019).

A complementary approach to behavioral experimentation, and one that may reveal new insights into underlying mechanisms, is to investigate how sensory information is integrated by individuals (i.e. via neural imaging). Since cockroaches are nocturnal animals, they rely heavily on their sense of smell to gain information about their surroundings—*e.g.*to locate food sources, sense conspecifics, potential danger, and to find mates (Bell et al., 2007). Olfactory cues are received by approx. 230,000 olfactory sensory neurons (OSNs) located on their antennae, and relayed to the antennal lobe (AL), the first odor processing center in the insect brain, analogous to the vertebrate olfactory bulb (Sass, 1983; Schafer and Sanchez, 1973). The cockroach AL comprises 200 anatomical and functional units, the glomeruli (Watanabe et al., 2010), which collect the input from the OSNs and forward it to higher-order brain centers by means of uniglomerular and multiglomerular projection neurons (PNs) (Malun et al., 1993; Watanabe et al., 2017). All sensory neurons bearing the same olfactory receptor project to a single glomerulus, converging onto the same uniglomerular PN. This parallel flow of information from cognate OSNs to uniglomerular PNs is cross-linked by a network of inhibitory local interneurons (LNs) (Distler, 1989), which interconnects multiple glomeruli and contributes to shaping the neural representation of an olfactory cue (Fusca et al., 2013; Husch et al., 2009; Olsen and Wilson, 2008; Silbering et al., 2008).

Here, we employed shelter selection as an assay to investigate the sensory basis of individual and collective decision-making in cockroaches (*Periplaneta americana*). We discover that the presence of a social odor influences individual shelter selection and monitor how food- and social-related olfactory information shape individual preference. To test how behavioral choices relate to the neural representation of the stimuli, we adopted a recently established method for selectively labeling the uniglomerular PNs population with a calcium sensitive dye for AL functional imaging (Paoli et al., 2020). Thus, combining neuroimaging with behavioral assays, we studied how food and colony odor cues, alone or combined, are encoded by the cockroach brain and how their perception guides behavioral choices.

Results

Inversion of shelter preference when in groups

Shelter preference was assessed from the behavior of individuals and groups of cockroaches in a circular arena with two opaque shelter options: one containing an olfactory cue and one unscented as a control (Figure 1A). Animals were tracked for 30 min to characterize individuals' behavior both outside and within the shelters (Figure 1B). During this time, cockroaches typically explored the arena and intermittently visited both shelters.

As previously documented (Sakura and Mizunami, 2001; Laurent Salazar et al., 2017), individual cockroaches show innate attraction to vanillin, and spent more time in close proximity to the vanillin shelter than to the unscented one (Figure 2A$_{ii}$). A similar trend, although weaker, could be observed also when the scented shelter contained lower vanillin concentration (Figure 2B and Supplemental information Appendix, Figure S1A$_{ii}$ n = 15 for each). However, when groups of cockroaches were tested together, the behavioral outcome was reversed, in agreement with the observation of (Laurent Salazar et al., 2017). In groups, individuals spent more time in and around the unscented control shelter compared to those that were tested individually (Figures 2A$_i$ and 2B; n = 10 groups, 20 individuals each).

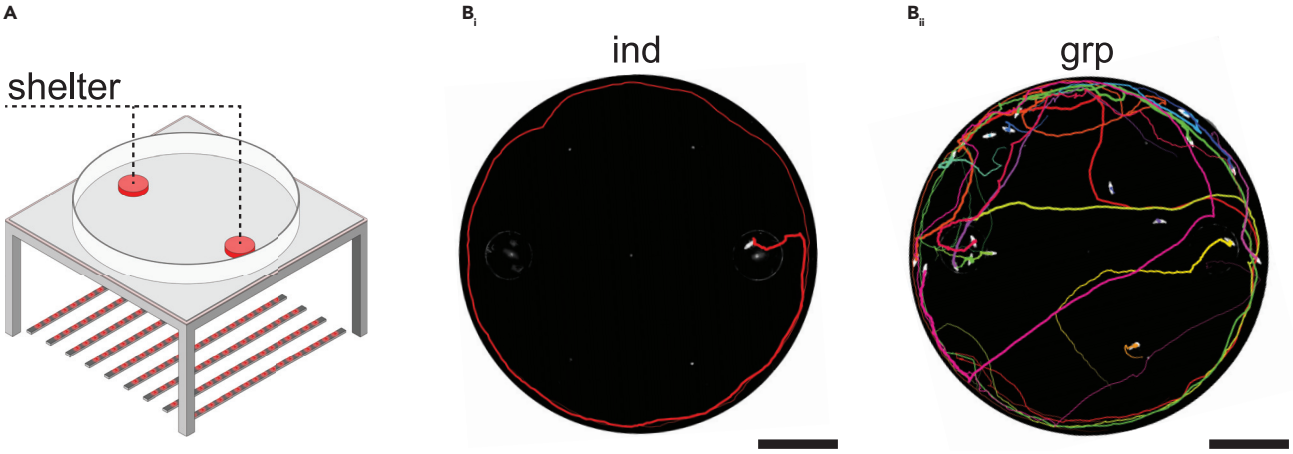

Figure 1. Experimental setup to record shelter selection of individuals or groups

(A) Schematic of the arena. Two shelters (d = 12 cm; h = 2 cm) were placed in randomly selected positions out of six possible locations for odor insertion. Shelters were always opposing each other. The arena (d = 90 cm) was illuminated using arrays of IR LEDs placed below and filmed from above with a Basler camera (not shown).

(B) A tracking software (modified from [Sridhar et al., 2019] to keep animal identities) was used to record animal trajectories in individual (B_i) and group trials (B_{ii}). Images were cropped and colors inverted to highlight the exemplary trajectories during a period of 60 s. Thickness of strokes codes time. Scale bars: 20 cm.

Density maps of the different tested conditions show the spatial distribution of individuals throughout trials, with the overall density along the two dimensions of the arena plotted in a solid line above and beside the heatmaps (Figure 2A and Supplemental information Appendix, Figure S1A for all other tested conditions). Note that while randomized in the experiments, all data presented are oriented to present the odor side on the right. Cockroaches were attracted to the shelters in all tested conditions and the direction of preference was quantified by the proportion of time (Figure 2B) and number of entries (Figure 2C) to the odor versus the control shelter. In particular, when facing the choice between vanillin and the unscented control in the individual assay, cockroaches clearly shifted their preference toward the vanillin shelter (individuals overall displayed significantly increased shelter (Figure 2B, p = 0.004) and entry (Figure 2C, p = 0.009) preference indices in comparison the the mean group level, one-sample two-tailed randomization tests).

When 20 individuals are tested together, despite the fact that cockroaches exhibit a higher propensity to aggregate in the control shelter (the likelihood of the vanillin shelter being empty (n = 0) is double than that of the unscented one [Figure 2D, blue/gray histogram shows the number of individuals at the vanillin/control shelter in all group trials]), we do not find evidence that individuals exhibit a different social tendency. For both shelters, cockroaches tend to remain longer (exhibit longer bouts) in shelters with higher occupancy, as long as they are not overcrowded, but this social relationship does not differ between the two shelters (Figure 2E, if anything overcrowding—or reduction in social feedback above a high occupancy limit—is more apparent in the control). This suggests that the increased group sizes found in the control shelter may not result solely from a decreased social attractivity in the presence of vanillin. A mutually not exclusive alternative possibility is that individuals exhibit an innate change in their shelter preference in the presence of social cues.

How social cues impact individual shelter preference

In order to better understand the basis of the preference inversion, we investigated how individual preference is influenced by social cues. We hypothesized that the presence of an odor of conspecifics would influence decisions of individuals and thus tested whether a similar inversion of preference is also observed when the only indication for conspecifics presence is a group-related smell. For this an extract of the colony feces was used as a social-related odor (Wada-Katsumata et al., 2015; Zhang et al., 2019) and added to the vanillin shelter at varying concentrations (fe2(3),van2+fe3, van2+fe2, van3+fe2; van2(3), vanillin dilution of $10^{-2(3)}$; fe2(3), feces extract dilution of $10^{-2(3)}$).

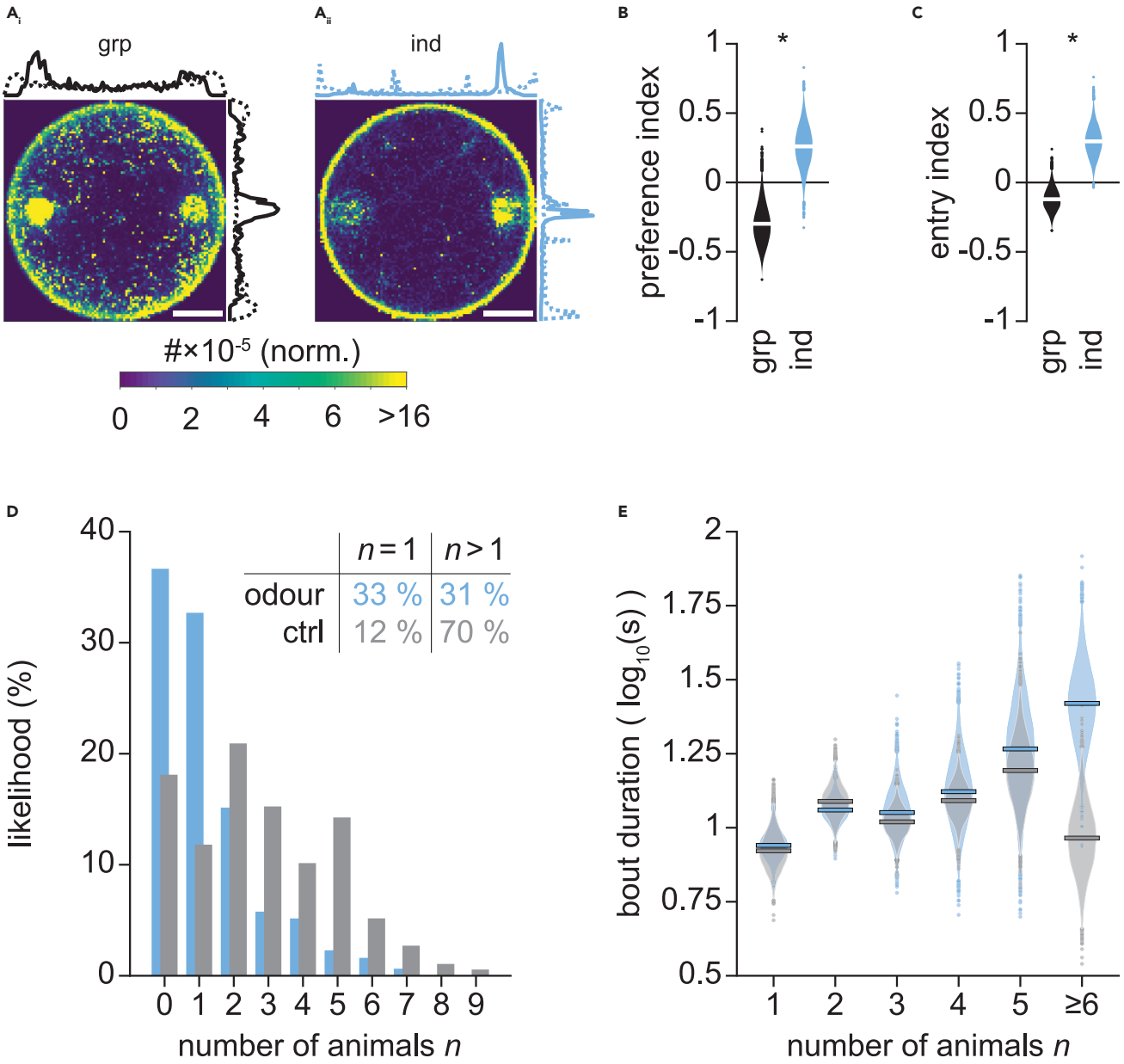

Figure 2. Shelter preference in individual and group trials

In all panels, vanillin diluted to 10^{-2} was administered to the odor shelter, while pure mineral oil was administered to the control shelter.

(A) Density maps of animal positions over all group (Ai) and individual (Aii) trials. Heatmaps show counts per pixel, normalized to 1 and averaged for the number of tested animals Presence densities across and along the arena are indicated above and beside the heatmaps. As wall-following bouts were highly prevalent in all tested conditions especially during the beginning of each trial, presence density was separated for the outer (wall-following bouts, dotted lines) and inner (solid lines) part of the arena. The sum of both yields the presence density for the whole arena. Scale bars: 20 cm.

(B) Shelter preference index based on the proportion of time individuals spend in the odor versus control (unscented) shelter, for group (black) and individual (blue) trials.

(C) Preference index based on entries to the odor vs. control shelter for groups and individuals. For both preference indices, a value of positive one indicates a complete preference for the odor shelter/quarter, while and a value of negative one a complete preference for the control shelter/quarter (for details see subsection Tracking and data analysis of the Transparent methods section). Asterisks indicate significant differences between distributions of individual trials and the mean group level($p < 0.05$), using a one-sample two-tailed randomization test.

Figure 2. *Continued*

(D) Probability histograms for the number of sheltered individuals in the odor (blue) and control (gray) shelters during group trials. The likelihood of observing a single animal, or a group of animals is not independent of the shelter (chi-squared test, $\chi^2 = 69.37$, $df = 1$, $p < 0.001$).

(E) Bout duration as a function of the average number of animals (rounded) sheltered during each stay, depicted as violin plots (as in D, blue and gray represent the odor and control shelters, respectively). Horizontal lines show distribution means. Values of six or more sheltered individuals are rare, especially for the odor shelter (see D), and grouped together. Abbreviations: grp, group; ind, individual; ctrl, control

We analyzed individuals' preferences for both for the shelters (Figure 3A) and also the area in close proximity of the shelters (splitting the arena into quarters, as shown in Figure 3B). The latter analysis was conducted because we observed that the shelter influences cockroach behavior when they are in its vicinity as well as within it. Both vanillin and social odor, when presented alone, are attractive. However, when presented together at one shelter, if the concentration of social odor is sufficiently high, individuals invert their preference, as seen in the group experiments (see Figure Figures 3$A_{ii}$and 3$B_{ii}$for the proportion of time spent in the odor (colored bar) and control (empty bar) shelter/quarter, respectively, and Supplemental information Appendix, Figure S1 for density maps across the arena in all tested conditions). For the duration of our experiments, we found that, over time, individuals exhibited intermittent visits to both shelters and their respective quarters, while their preferences remained consistent (Figures 3$A_{iii}$and 3B_{iii}). This allowed us to determine a single preference index (the relative time in the odor vs. control shelter/quarter) for each condition (Figures 3A_{iv} and 3B_{iv}).

Tracking of individual cockroaches allowed us to evaluate the relative proportion of entries into the odor and the control shelter for each condition. For each condition, individuals were found to enter more frequently their shelter of preference (Figures 4A_{ii} and 4A_{iii}). In addition, the time spent in the shelter for each visit (bout duration) was longer in the preferred shelter (Figures 4$B_{ii}$and 4$_{iii}$). This demonstrates that both the probability of visiting a shelter, as well as the duration of stay during each visit, contribute to the overall time spent by individuals in each shelter, and thus to the observed differences in shelter preference.

Taking into account the different behavioral features shown in Figures 3 and 4, behavioral similarity across all tested conditions was evaluated using a hierarchical clustering algorithm, indicating that the behavior of individuals in the group context are overall similar to isolated individuals, when vanillin is combined with a social odor component (Figure 4C, red boxes).

Colony odor modulates vanillin-induced response in the AL

To investigate how the observed preferences relate to the neural representation of the stimuli, we employed calcium imaging to determine how vanillin, feces extract, and mixtures of the two, are mapped in the primary olfactory center of the cockroach, the AL. Following a recently developed protocol (Paoli et al., 2020), uniglomerular PNs were selectively labeled with the calcium sensor Fura-2 for functional imaging analysis. Successful labeling resulted in bright fluorescence of the PNs somata clusters as well as their uniglomerular dendritic arborizations, allowing several hours of calcium imaging analysis per individual ($n = 10$) with multiple olfactory stimulation sessions (Figure 5A; Paoli et al., 2020). Hence, we tested the same odor combinations employed in the behavioral assays and analyzed their neural representations.

During odor presentation, changes in intracellular calcium levels could be observed in discrete areas comparable in size and shape to individual glomeruli (Figures 5A and 5B). Individuals exhibited stimulus-dependent glomerular response maps that were consistent across repetitions (Figure 5C, see also Supplemental information Appendix, Figures S2 and S3). As no difference in response latency was observed across the different stimuli (Supplemental information Appendix, Figures S2B and S3B), all analyses were based on the average odor response maps between 0.6 and 1 s after stimulus onset (when the calcium-induced responses were strongest) across three-to-four non-consecutive repetitions of the same stimulus after subtracting the response to the solvent, *i.e.*mineral oil. For further details on calcium signal analysis, see Transparent methods section.

Response intensity increased with increasing stimulus concentrations. At a higher concentration (10^{-2} dilution), both vanillin and feces extract induce calcium responses in multiple areas of the AL with stimulus-specific activity maps (responses to 10^{-3} dilutions were weak across all regions and therefore not included in

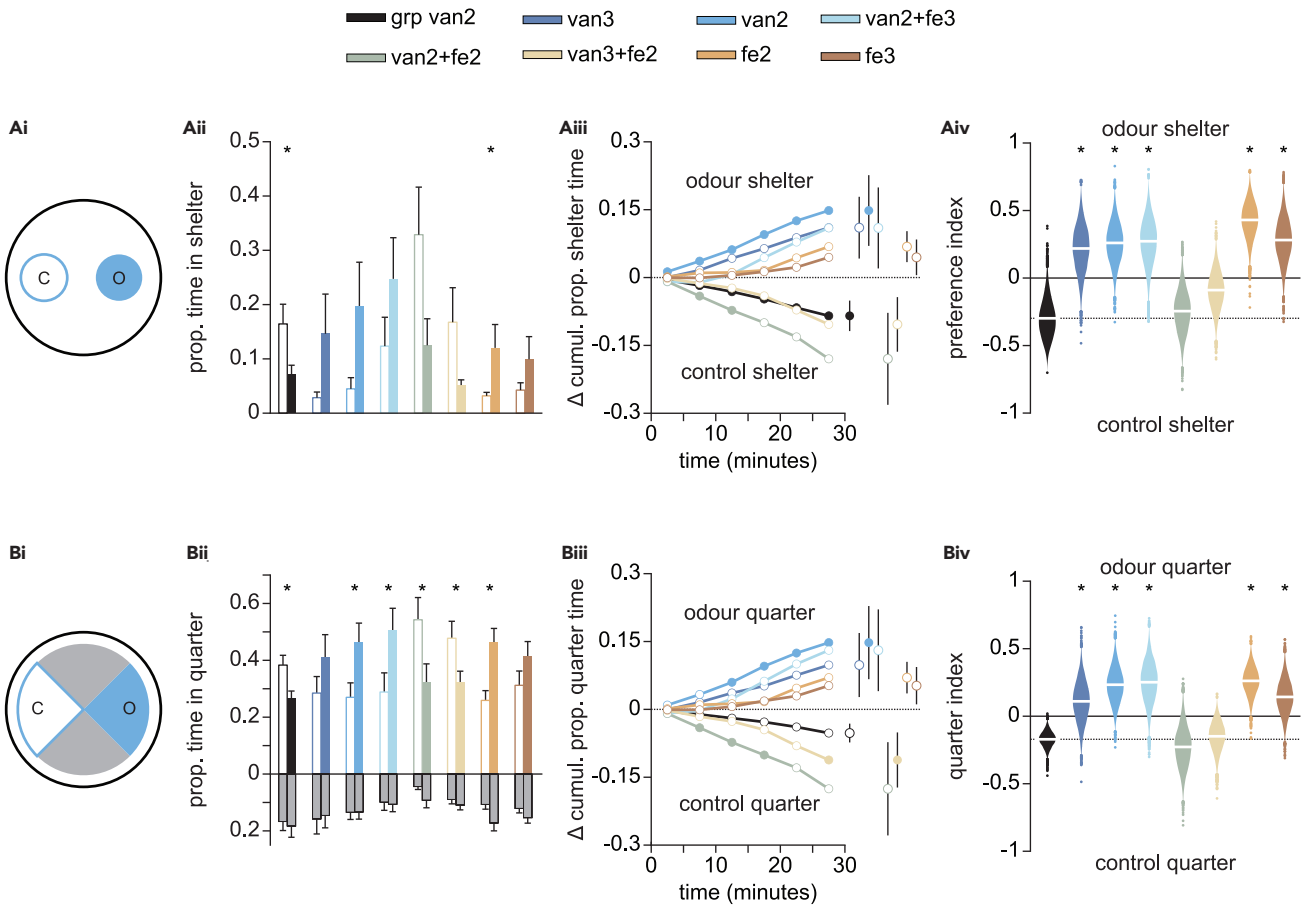

Figure 3. Individual preference is inverted in an olfactory simulated group context

Proportion of time in the shelters (A) and in the four different quarters (B) of the arena. (A_{ii}) and (B_{ii}) show the proportion of time in the odor (full bars) and control (empty bars) shelter/quarter. Error bars denote standard deviations and asterisks statistically significant differences ($p < 0.05$) between proportion of time in the odor vs. control shelter/quarter, using a two-sample two-tailed randomization test. In (B) upright bars above the x axis represent the odor and control quarters and the inverted correspond to the empty quarters. (A_{iii}) and (B_{iii}) The difference in the cumulative proportion of time in the odor vs. the control shelter/quarter for each tested condition. The differences in cumulative time were calculated in six bins of five minutes each. Standard deviation around the means of the last time bins are shown on the right of the line plots. Filled circles in (A_{iii}) and (B_{iii}) indicate a statistically significant difference between odor and control shelter/quarter ($p < 0.05$) using a two-sample two-tailed randomization test. (A_{iv}) and (B_{iv}) Preference index calculated based on the total time in the odor vs. control shelter/quarter for all eight conditions, based on the proportions shown in (A_{ii}) and (B_{ii}). A value of +1 indicates a complete preference for the odor shelter/quarter, while and a value of −1 a complete preference for the control shelter/quarter (for details see subsection Tracking and data analysis of the Transparent methods section). White horizontal lines show distribution means. Asterisks indicate statistically significant differences ($p < 0.05$) testing the distributions of the seven individual conditions against the mean level of the group condition (dotted line, obtained from the group experiments shown in Figure 2), using a one-sample two-tailed randomization test. Abbreviations: grp, group; van2(3), vanillin dilution of $10^{-2(3)}$; fe2(3), feces extract dilution of $10^{-2(3)}$.

the analysis). The presentation of both feces extract and vanillin together resulted in response maps similar to those elicited by the single components, depending on their relative concentration. The van10^{-2} + fe10^{-3} mixture produced a glomerular activation pattern similar to the one elicited by vanillin alone, while the balanced and the low-vanillin mixtures (van10^{-2} + fe10^{-2}, and van10^{-3} + fe10^{-2}) showed response profiles comparable to the one of feces extract alone. To quantitatively assess the physiological similarity among stimulus-induced responses, we calculated the correlation coefficients among odor response maps (Guerrieri et al., 2005; Paoli et al., 2020). For each animal and stimulus condition, we constructed a response vector considering all functional units activated by any of the odor conditions, segmented into 25 regions of interests (ROIs) using a *k*-medoids functional clustering algorithm (see Transparent methods section, examples for the first two animals in Figures 5B–5D, and more in details in Supplemental information Appendix, Figures S2–S4). Response vectors were used to calculate the correlation matrix across

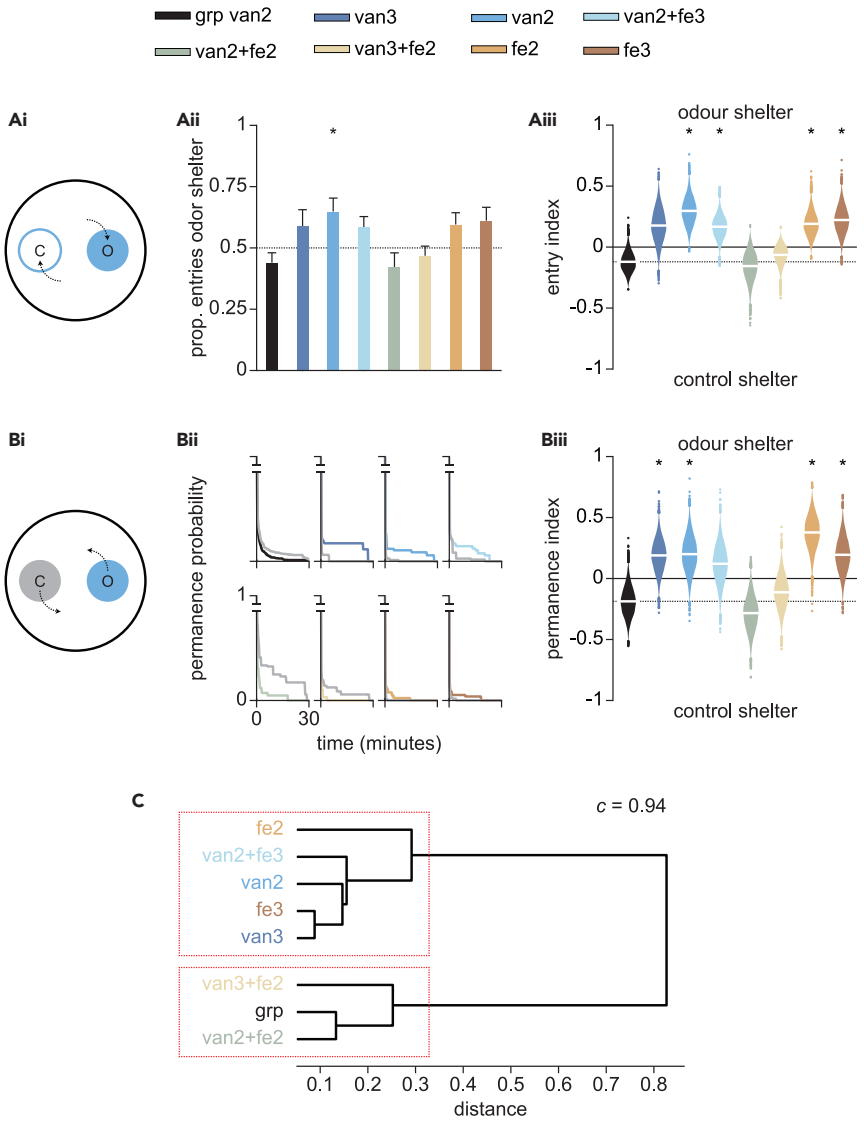

Figure 4. Shelter selection behavior is odor-dependent

(A) The proportion of entries (A_{ii}) for the odor vs. control shelter and resultant entry index (A_{iii}) for the eight tested conditions.

(B) Permanence probability (based on bout duration per visit) for each tested condition in the odor (color) and control (gray) shelters. Integrals of permanence probability curves were used to calculate the permanence index in B_{iii} (see Transparent methods section for details). In both A_{iii} and B_{iii} a value of positive one indicates a complete preference for the odor shelter, while and a value of negative one a complete preference for the control shelter (for details see subsection Tracking and data analysis of the Transparent methods section). White horizontal lines show distribution means. Asterisks indicate statistically significant differences ($p < 0.05$) of testing the distributions against chance level (0.5) in $A_{ii}$and comparing distributions of individual trials with the mean level of the group in A_{iii} and B_{iii} (dotted lines), using one-sample two-tailed tests.

(C) Similarity among conditions is depicted as a dendrogram of the hierarchical binary cluster tree, resulting from the Euclidean distances between groups. Data used are (I) shelter and (ii) quarter preference index, (iii) entry index and (iv) permanence index. The cophenetic correlation coefficient ($c = 0.94$) was used to evaluate the clustering. Abbreviations: grp, group; van2(3), vanillin dilution of $10^{-2(3)}$; fe2(3), feces extract dilution of $10^{-2(3)}$.

conditions and quantify odor response similarity (Figure 5E and Supplemental information Appendix, Figure S4 for correlation matrices of individual animals, and Figure 5G for the same analysis considering all ROIs for all individuals).

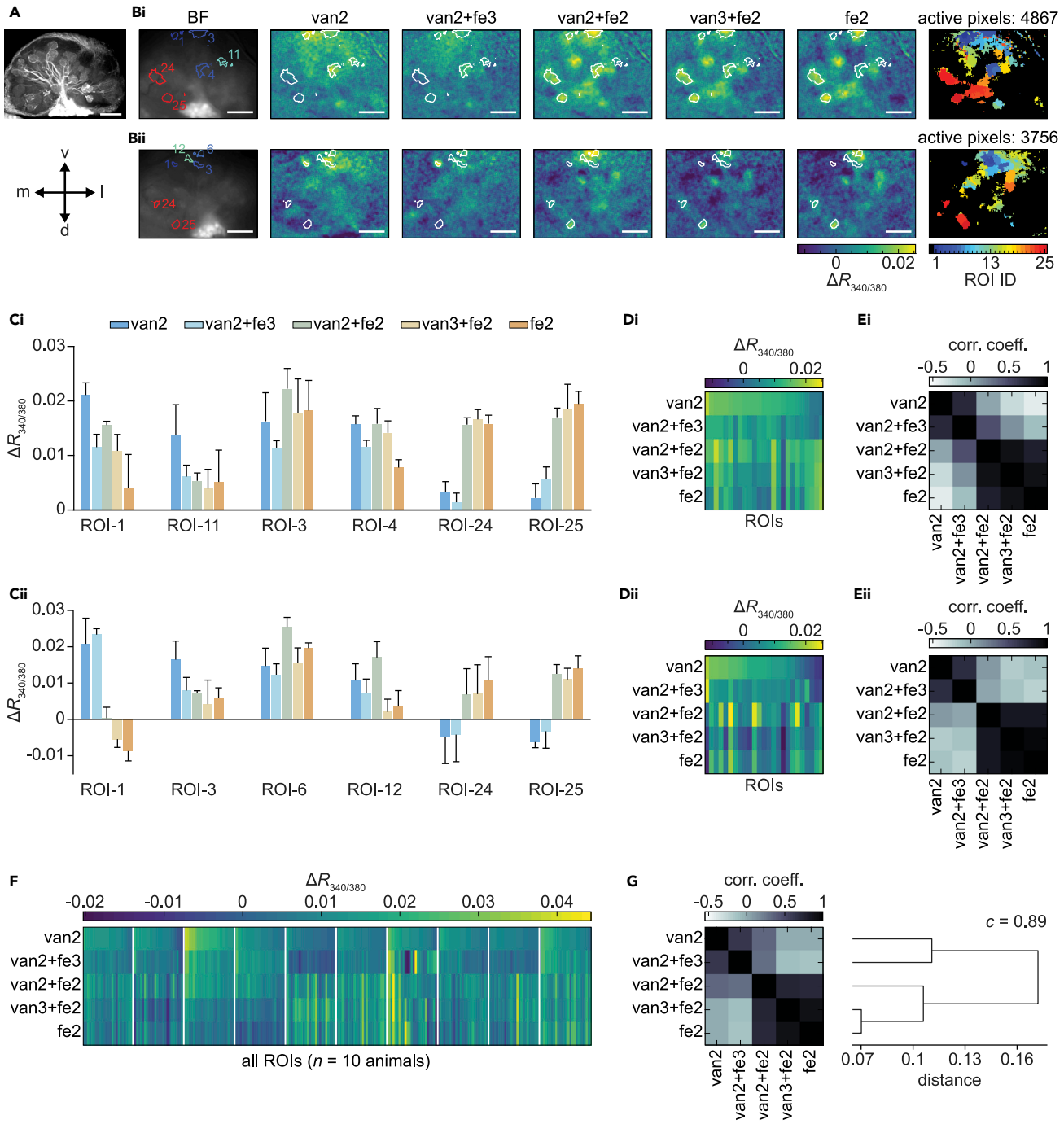

Figure 5. Calcium imaging analysis of antennal lobe representations of tested odorants

(A) A confocal image of the right AL with labeled uniglomerular PNs.

(B) Antennal lobe bright field microscopy image (greyscale), false color-coded images of the AL after olfactory stimulation, and distribution of ROIs resulting from *k*-medoids clustering on active pixels (¿0.01 $\Delta R_{340/380}$ for at least one of the five odors) for two representative individuals. ROI identities were sorted by vanillin (van2)-responsiveness. Numbers within the bright field image indicate selected exemplary ROIs displayed in panels (C) and (D). Each response intensity map is the average response pattern of 4 repetitions of the same stimulus. Scale bars in (A) and (B), 100 μm.

(C) For the six representative ROIs, the mean response intensity ±SEM (n = 4 repetitions) to the five olfactory stimuli is shown.

(D) Mean response intensities (n = 4 repetitions) of all ROIs activated by any of the five olfactory stimuli are plotted as odor response vectors.

(E) Similarity matrix based on the Pearson's correlation coefficient among response vectors from (D).

(F) Glomerular response vectors from ten cockroaches were combined into a meta-response matrix (n = 10 animals, 250 ROIs, 25 ROIs per animal).

Figure 5. *Continued*

(G) Pearson's correlation coefficient matrix and hierarchical dendrogram calculated for response vectors plotted in (F). The cophenetic correlation coefficient (c = 0.89) was used to evaluate the clustering. Abbreviations: BF, bright field; v, ventral; l, lateral; d, dorsal; m, medial; grp, group; van2(3), vanillin $10^{-2}(10^{-3})$; fe2(3), feces extract 10^{-2} (10^{-3}); ROIs, regions of interest.

As can be seen in the dendrogram, which considers all individuals, the neural representation of vanillin in the glomerular space shifts closer to that one of feces extract as the proportion of the latter in the mixture increases (Figure 5G). When concentration of both vanillin and social odor are high, we find that the latter is dominant (but not exclusive), with only weak activity being observed in the vanillin-sensitive regions (Figure 5G, Supplemental information Appendix, Figure S4). This finding suggests that the way in which vanillin is perceived is different in a social context, and that this perceptual difference could contribute to the observed preference inversion in the behavioral experiments.

Discussion

Isolated cockroaches show an innate preference for vanillin-scented versus unscented shelters, a preference that is reversed in the presence of conspecifics (Figures 2, 3, and 4, Laurent Salazar et al., 2017; Martín et al., 2019). Previously, it was proposed that this type of inversion results from a weakening of the social attraction in the individually preferred shelter (in this case vanillin) (Laurent Salazar et al., 2017; Martín et al., 2019). In our experiments, we found that the propensity to stay in a shelter increases with the number of conspecifics present (a proxy of social attractivity), but this relationship does not differ in the presence of vanillin. Subsequently we show that this preference switch also occurs when the social context is replaced by social odor (colony feces extract) alone, demonstrating that olfaction is a key (and sufficient) modality for inducing the preference inversion.

The balanced mixture has an intermediate neural representation with respect to its two components, although closer to the social odor representation. Still, the observation of a preference inversion for the food-social odor mixture—with respect to both components—suggests that it is evaluated synthetically, *i.e.* as a different olfactory object, with a valence that is different from the one of its elemental components. In the context of foraging, which may also be relevant for shelter selection given that food presence increases shelter attractivity, social feedback can act both as a negative or a positive reinforcer, balancing foraging efficiency, and flexibility in mass-recruiting insect colonies (Grueter et al., 2012). Alone, both the vanillin and the social odor increase shelter attractivity, but together they provide a negative feedback. Ecologically, these observations are consistent with the possibility that individuals utilize social cues to avoid what they perceive as recently depleted resources (since the presence of social odor will likely be correlated with the current, or relatively recent, presence of conspecifics).

AL calcium imaging (Figure 5) shows that vanillin and social odor elicit activation in distinct but partially overlapping regions. When presented together, their relative concentrations influence the neural representation of the mixture, shifting it closer to the activity map elicited by the dominant component. In those conditions that promoted reduced preference for the odor shelter, vanillin-specific glomeruli were less responsive, while social odor regions showed stronger activation—in some cases even higher than for the pure component alone (*i.e.* ROI-6 and ROI-12 in Figure 5C_{ii}, and examples 3, 4, and 7 in the Supplemental information Appendix, Figure S3). It is still to be determined if this effect (and the resulting behavior) depends on a glomerular cross-talk within the AL, or if the glomerular representation of the mixture is further processed in higher-order brain areas (*e.g.* the lateral horn [LH]) and evaluated as an olfactory object different from its two elemental components.

While odor valence evaluation in cockroaches is still understudied, research on other insects—and notably in *Drosophila* - has found that valence can be encoded already at the level of the AL. A study of AL olfactory coding in the fruit fly showed that even if an ensemble of OSNs has no detectable valence specificity, analysis of the elicited glomerular response maps allows valence-based odor classification (Knaden et al., 2012; Knaden and Hansson, 2014). This suggests that, at least in the fruit fly, the AL may dedicate different glomerular populations for attractive and aversive odorants, and that the network of LNs may process OSNs input to enhance valence classification already at the periphery of the olfactory circuit (Niewalda et al., 2011; Knaden et al., 2012; Knaden and Hansson, 2014). AL output neurons relay olfactory information to the mushroom body and LH. The former has a neuronal layout that favors a sparse odor coding, meaning that two odors are encoded by different subsets of intrinsic neurons with little overlapping. This is a very

different coding strategy with respect to the AL (where many glomeruli respond to many odorants with a high overlap among the response maps elicited by two stimuli) and provides an efficient neuronal substrate for odor recognition, discrimination, and learning. On the other hand, the LH is innervated without reshaping olfactory information, meaning that distances among PN pre-synaptic response maps elicited in the LH by different odorants are comparable to the distances among the odor response maps induced by the same stimuli in the AL glomerular space (Roussel et al., 2014; Frechter et al., 2019). Moreover, recent neuroanatomical observations have shown that PNs from the same or similarly tuned glomeruli, tend to converge on the same LH output neuron (Jeanne et al., 2018; Frechter et al., 2019). Hence, PN-LH connectivity partially collapses the olfactory space clustering odors by structural and, to some extent, perceptual similarity (Sachse et al., 1999; Guerrieri et al., 2005), providing a good substrate for innate odorant classification. This arrangement suggests that even though overall LH neurons show higher specificity in olfactory stimuli classification and higher capacity to encode complex odor features than AL neurons (Frechter et al., 2019), it cannot be excluded that initial valence evaluation could occur already within the AL. Recent investigation of the cockroaches olfactory coding principles have shown that chemical features of single molecules, such as carbon chain length, maintain a topological mapping within the AL (Paoli et al., 2020), suggesting that coding rules may be similar to other insects (Sachse et al., 1999; Couto et al., 2005) and vertebrates (Uchida et al., 2000). Hence, it is possible that the valence of food, colony, and their mixtures undergoes a first evaluation in the AL and that an activity change in vanillin-responsive glomeruli when presented together with the colony odor may result in a behavioral preference inversion.

In nature, insects rarely encounter monomolecular odorants, and the AL representations of odorant mixtures can be dominated by either a salient component, or can acquire a new quality and become an olfactory object cognitively different from its constituent components (Renou, 2014; Silbering and Galizia, 2007; Thoma et al., 2014). In general, valences of binary mixtures reflect the combined valence of the components. Two attractants (or repellents) combined are often more attractive (or repulsive) than the individual mixture constituents. In the fruit fly, for example, the presence of vinegar scent together with the male sexual pheromone modulates the AL representation of the latter, making a virgin female more sensitive to the pheromone, thus enhancing her receptivity during courtship (Das et al., 2017). Blends of odors with opposing valences, instead, often elicit concentration-dependent intermediate responses, which are mediated by cross-talk interactions between glomeruli responding to the individual components (Thoma et al., 2014; Mohamed et al., 2019). In these cases, glomeruli that strongly responded to the attractive component were shown to be inhibited by the aversive one, thus providing an instance where the processing of conflicting inputs occurs already within the AL, with a direct influence on the behavioral output; whereas those two cases reported the enhancement of a positive stimulus within a mixture of two attractants (Das et al., 2017) or the weakening of an attractant in presence of a repellant (Mohamed et al., 2019), here, we observed that a mixture is evaluated with the opposite valence with respect to its elemental components.

Modulation of the neural representation of olfactory stimuli in the AL plays an important role in mediating fundamental behaviors. The above-mentioned example of synergistic interactions between pheromone sensitive PNs and food-responsive glomeruli to increase mating receptivity in presence of food were reported both in flies (Das et al., 2017) and moths (Light et al., 1993; Namiki et al., 2008). During starvation, AL modulation has been shown to result in an increase in sensitivity to attractive odors and a decrease response to aversive ones, thus increasing nutrient detection capability at the risk of ignoring potentially toxic resources (Ko et al., 2015). Aligned with these studies, the observed reduction in vanillin-shelter preference induced by the social cue, is paralleled with an altered neural representation of vanillin in the AL, the first relay of odor processing, which may advocate for its ecological prominence.

The possibility of replicating social behavior by utilizing social odor alone can facilitate a systematic study of how food and social cues jointly influence individual decision-making. Further studies are necessary to elucidate the cellular mechanisms involved. In addition, it will be important to evaluate both the ubiquity, and the ecological value, of preference inversion, which may be an important strategy to exploit resources in unpredictable and patchy environments.

Limitations of the study

Our study investigates the influence of a social environment on individual decisions. It shows that an increasing concentration of a social odor—an otherwise attractive stimulus—resulted in a reduced

preference for a vanillin-associated shelter, supported by a change in the neural representation of the different stimuli. Therefore, we suggest that a synthetic perception of the intermediate mixture—perceived as a third object with respect to its elemental components—provides the basis for a different evaluation of odor valence, which mediates the observed behavioral inversion. At this stage, however, it cannot prove causality. In addition, an intrinsic limitation of our imaging procedure is that it allows access only to the superficial glomeruli of the AL. A full decryption of the AL representation of the odor mixture would require the use of 2-photon microscopy to image deeper layers. Further experiments to test behavioral choices and related AL activity will be needed to determine if the observed phenomenon is general to other important food odors in combination with a social odor. Computational modeling of this behavior would also be valuable to create testable predictions regarding the consequences of the observed inversion across spatial and temporal scales. It could be addressed whether this is a strategy for competition avoidance, whether it is a general strategy for social organisms that live in patchy environments, and whether it has adaptive implications.

Resource availability

Lead contact

Further information and questions should be directed to and will be fulfilled by the lead contact, Einat Couzin-Fuchs (einat.couzin@uni-konstanz.de).

Materials availability

No new materials were generated in this study.

Data and code availability

Code used for data analysis and Figure creation is available at https://github.com/Couzin-Fuchs-Lab/Guenzel-McCollum-et-al. Raw data are available on request.

Methods

All methods can be found in the accompanying Transparent methods supplemental file.

Supplemental information

Supplemental Information can be found online at https://doi.org/10.1016/j.isci.2020.101964.

Acknowledgments

The authors thank Prof. Hiroshi Nishino for providing the feces extract as well as a general advice along the way; Iain Couzin for his valuable feedback on the manuscript; Antoine Hoffmann for helpful comments on data analysis; Margarete Ehrenfried for rearing *P. americana*. We also thank Alina Hebling, Hannah Honner and Jahn Nitschke for help with experiments and analysis. The authors thank the 4 anonymous reviewers for their insightful suggestions. This work was completed with the support of the Deutsche Forschungsgemeinschaft (DFG, German Research Foundation) under Germany's Excellence Strategy – EXC 2117–422037984.

Author contributions

J.M., M.P., and E.C.-F. designed the study; J.M., M.P., and I.P. performed experiments; G.G. guided calcium imaging; Y.G. and M.P. performed the data analysis, and curated data availability and reproducibility; E.C.-F. supervised the overall data collection and analysis; All authors contributed to the manuscript writing.

Declaration of interests

The authors declare no competing interests.

Received: August 17, 2020
Revised: September 24, 2020
Accepted: December 15, 2020
Published: January 22, 2021

References

Amé, J.-M., Halloy, J., Rivault, C., Detrain, C., and Deneubourg, J.L. (2006). Collegial decision making based on social amplification leads to optimal group formation. Proc. Natl. Acad. Sci. U S A *103*, 5835–5840.

Ame, J.-M., Rivault, C., and Deneubourg, J.-L. (2004). Cockroach aggregation based on strain odour recognition. Anim. Behav. *68*, 793–801.

Bell, W.J., Roth, L.M., and Nalepa, C.A. (2007). Cockroaches: Ecology, Behavior, and Natural History (JHU Press).

Canonge, S., Deneubourg, J.-L., and Sempo, G. (2011). Group living enhances individual resources discrimination: the use of public information by cockroaches to assess shelter quality. PLoS One *6*, e19748.

Canonge, S., Sempo, G., Jeanson, R., Detrain, C., and Deneubourg, J.L. (2009). Self-amplification as a source of interindividual variability: shelter selection in cockroaches. J. Insect Physiol. *55*, 976–982.

Couto, A., Alenius, M., and Dickson, B.J. (2005). Molecular, anatomical, and functional organization of the drosophila olfactory system. Curr. Biol. *15*, 1535–1547.

Das, S., Trona, F., Khallaf, M.A., Schuh, E., Knaden, M., Hansson, B.S., and Sachse, S. (2017). Electrical synapses mediate synergism between pheromone and food odors in drosophila melanogaster. Proc. Natl. Acad. Sci. U S A *114*, E9962–E9971.

Distler, P. (1989). Histochemical demonstration of gaba-like immunoreactivity in cobalt labeled neuron individuals in the insect olfactory pathway. Histochemistry *91*, 245–249.

Doi, N., and Toh, Y. (1992). Modification of cockroach behavior to environmental humidity change by dehydration (dictyoptera: Blattidae). J. Insect Behav. *5*, 479–490.

Dunlap, A.S., Nielsen, M.E., Dornhaus, A., and Papaj, D.R. (2016). Foraging bumble bees weigh the reliability of personal and social information. Curr. Biol. *26*, 1195–1199.

Durier, V., and Rivault, C. (2000). Learning and foraging efficiency in German cockroaches, blattella germanica (l.)(insecta: dictyoptera). Anim. Cogn. *3*, 139–145.

Frechter, S., Bates, A.S., Tootoonian, S., Dolan, M.-J., Manton, J., Jamasb, A.R., Kohl, J., Bock, D., and Jefferis, G. (2019). Functional and anatomical specificity in a higher olfactory centre. Elife *8*, e44590.

Fusca, D., Husch, A., Baumann, A., and Kloppenburg, P. (2013). Choline acetyltransferase-like immunoreactivity in a physiologically distinct subtype of olfactory nonspiking local interneurons in the cockroach (periplaneta americana). J. Comp. Neurol. *521*, 3556–3569.

Grueter, C., Schuerch, R., Czaczkes, T.J., Taylor, K., Durance, T., Jones, S.M., and Ratnieks, F.L. (2012). Negative feedback enables fast and flexible collective decision-making in ants. PLoS One *7*, e44501.

Guerrieri, F., Schubert, M., Sandoz, J.-C., and Giurfa, M. (2005). Perceptual and neural olfactory similarity in honeybees. PLoS Biol. *3*, e60.

Hall, C.L., and Kramer, D.L. (2008). The economics of tracking a changing environment: competition and social information. Anim. Behav. *76*, 1609–1619.

Husch, A., Paehler, M., Fusca, D., Paeger, L., and Kloppenburg, P. (2009). Calcium current diversity in physiologically different local interneuron types of the antennal lobe. J. Neurosci. *29*, 716–726.

Jeanne, J.M., Fişek, M., and Wilson, R.I. (2018). The organization of projections from olfactory glomeruli onto higher-order neurons. Neuron *98*, 1198–1213.

Jeanson, R., Rivault, C., Deneubourg, J.-L., Blanco, S., Fournier, R., Jost, C., and Theraulaz, G. (2005). Self-organized aggregation in cockroaches. Anim. Behav. *69*, 169–180.

Kendal, R., and Collen, I. (2011). 13 Adaptive Trade-Offs in the Use of Social and Personal Information.

Kendal, R.L., Coolen, I., and Laland, K.N. (2004). The role of conformity in foraging when personal and social information conflict. Behav. Ecol. *15*, 269–277.

King, A.J., and Cowlishaw, G. (2007). When to use social information: the advantage of large group size in individual decision making. Biol. Lett. *3*, 137–139.

Knaden, M., and Hansson, B.S. (2014). Mapping odor valence in the brain of flies and mice. Curr. Opin. Neurobiol. *24*, 34–38.

Knaden, M., Strutz, A., Ahsan, J., Sachse, S., and Hansson, B.S. (2012). Spatial representation of odorant valence in an insect brain. Cell Rep. *1*, 392–399.

Ko, K.I., Root, C.M., Lindsay, S.A., Zaninovich, O.A., Shepherd, A.K., Wasserman, S.A., Kim, S.M., and Wang, J.W. (2015). Starvation promotes concerted modulation of appetitive olfactory behavior via parallel neuromodulatory circuits. Elife *4*, e08298.

Laurent Salazar, M.-O., Nicolis, S.C., Calvo Martín, M., Sempo, G., Deneubourg, J.-L., and Planas-Sitjà, I. (2017). Group choices seemingly at odds with individual preferences. R. Soc. open Sci. *4*, 170232.

Light, D.M., Flath, R.A., Buttery, R.G., Zalom, F.G., Rice, R.E., Dickens, J.C., and Jang, E.B. (1993). Host-plant green-leaf volatiles synergize the synthetic sex pheromones of the corn earworm and codling moth (lepidoptera). Chemoecology *4*, 145–152.

Lihoreau, M., Costa, J., and Rivault, C. (2012). The social biology of domiciliary cockroaches: colony structure, kin recognition and collective decisions. Insectes Sociaux *59*, 445–452.

Lihoreau, M., and Rivault, C. (2011). Local enhancement promotes cockroach feeding aggregations. PloS One *6*, e22048.

Malun, D., Waldow, U., Kraus, D., and Boeckh, J. (1993). Connections between the deutocerebrum and the protocerebrum, and neuroanatomy of several classes of deutocerebral projection neurons in the brain of male periplaneta americana. J. Comp. Neurol. *329*, 143–162.

Martín, M.C., Nicolis, S.C., Planas-Sitjà, I., and Deneubourg, J.-L. (2019). Conflictual influence of humidity during shelter selection of the american cockroach (periplaneta americana). Sci. Rep. *9*, 1–11.

Meyer, H., and Norris, D. (1967). Vanillin and syringaldehyde as attractants for scolytus multistriatus (coleoptera: Scolytidae). Ann. Entomol. Soc. Am. *60*, 858–859.

Miller, N., Garnier, S., Hartnett, A.T., and Couzin, I.D. (2013). Both information and social cohesion determine collective decisions in animal groups. Proc. Natl. Acad. Sci. U S A *110*, 5263–5268.

Mohamed, A.A., Retzke, T., Chakraborty, S.D., Fabian, B., Hansson, B.S., Knaden, M., and Sachse, S. (2019). Odor mixtures of opposing valence unveil inter-glomerular crosstalk in the drosophila antennal lobe. Nat. Commun. *10*, 1–17.

Namiki, S., Iwabuchi, S., and Kanzaki, R. (2008). Representation of a mixture of pheromone and host plant odor by antennal lobe projection neurons of the silkmoth bombyx mori. J. Comp. Physiol. A *194*, 501–515.

Niewalda, T., Völler, T., Eschbach, C., Ehmer, J., Chou, W.-C., Timme, M., Fiala, A., and Gerber, B. (2011). A combined perceptual, physico-chemical, and imaging approach to â€˜odour-distances' suggests a categorizing function of the drosophila antennal lobe. PLoS One *6*, e24300.

Olsen, S.R., and Wilson, R.I. (2008). Lateral presynaptic inhibition mediates gain control in an olfactory circuit. Nature *452*, 956–960.

Paoli, M., Nishino, H., Couzin-Fuchs, E., and Galizia, C.G. (2020). Coding of odour and space in the hemimetabolous insect periplaneta americana. J. Exp. Biol. *223*, jeb218032.

Planas-Sitja, I., Deneubourg, J.-L., Gibon, C., and Sempo, G. (2015). Group personality during collective decision-making: a multi-level approach. Proc. R. Soc. B: Biol. Sci. *282*, 20142515.

Renou, M. (2014). Pheromones and General Odor Perception in Insects (Neurobiology of chemical communication), p. 23.

Rieucau, G., and Giraldeau, L.-A. (2011). Exploring the costs and benefits of social information use: an appraisal of current experimental evidence. Philosophical Trans. R. Soc. B Biol. Sci. *366*, 949–957.

Roussel, E., Carcaud, J., Combe, M., Giurfa, M., and Sandoz, J.-C. (2014). Olfactory coding in the honeybee lateral horn. Curr. Biol. *24*, 561–567.

Sachse, S., Rappert, A., and Galizia, C.G. (1999). The spatial representation of chemical structures in the antennal lobe of honeybees: steps towards the olfactory code. Eur. J. Neurosci. *11*, 3970–3982.

Sakura, M., and Mizunami, M. (2001). Olfactory learning and memory in the cockroach periplaneta americana. Zool. Sci. *18*, 21–28.

Sass, H. (1983). Production, release and effectiveness of two female sex pheromone components ofperiplaneta americana. J. Comp. Physiol. *152*, 309–317.

Schafer, R., and Sanchez, T.V. (1973). Antennal sensory system of the cockroach, periplaneta americana: postembryonic development and morphology of the sense organs. J. Comp. Neurol. *149*, 335–353.

Silbering, A.F., and Galizia, C.G. (2007). Processing of odor mixtures in the drosophila antennal lobe reveals both global inhibition and glomerulus-specific interactions. J. Neurosci. *27*, 11966–11977.

Silbering, A.F., Okada, R., Ito, K., and Galizia, C.G. (2008). Olfactory information processing in the drosophila antennal lobe: anything goes? J. Neurosci. *28*, 13075–13087.

Sridhar, V.H., Roche, D.G., and Gingins, S. (2019). Tracktor: image-based automated tracking of animal movement and behaviour. Methods Ecol. Evol. *10*, 815–820.

Thoma, M., Hansson, B.S., and Knaden, M. (2014). Compound valence is conserved in binary odor mixtures in drosophila melanogaster. J. Exp. Biol. *217*, 3645–3655.

Torney, C., Neufeld, Z., and Couzin, I.D. (2009). Context-dependent interaction leads to emergent search behavior in social aggregates. Proc. Natl. Acad. Sci. U S A *106*, 22055–22060.

Uchida, N., Takahashi, Y.K., Tanifuji, M., and Mori, K. (2000). Odor maps in the mammalian olfactory bulb: domain organization and odorant structural features. Nat. Neurosci. *3*, 1035–1043.

Wada-Katsumata, A., Zurek, L., Nalyanya, G., Roelofs, W.L., Zhang, A., and Schal, C. (2015). Gut bacteria mediate aggregation in the German cockroach. Proc. Natl. Acad. Sci. U S A *112*, 15678–15683.

Watanabe, H., Nishino, H., Mizunami, M., and Yokohari, F. (2017). Two parallel olfactory pathways for processing general odors in a cockroach. Front. Neural Circuits *11*, 32.

Watanabe, H., Nishino, H., Nishikawa, M., Mizunami, M., and Yokohari, F. (2010). Complete mapping of glomeruli based on sensory nerve branching pattern in the primary olfactory center of the cockroach periplaneta americana. J. Comp. Neurol. *518*, 3907–3930.

Zhang, J., Bisch-Knaden, S., Fandino, R.A., Yan, S., Obiero, G.F., Grosse-Wilde, E., Hansson, B.S., and Knaden, M. (2019). The olfactory coreceptor ir8a governs larval feces-mediated competition avoidance in a hawkmoth. Proc. Natl. Acad. Sci. U S A *116*, 21828–21833.

iScience, Volume *24*

Supplemental Information

Social modulation of individual preferences in cockroaches

Yannick Günzel, Jaclyn McCollum, Marco Paoli, C. Giovanni Galizia, Inga Petelski, and Einat Couzin-Fuchs

Supplementary Information for

Supporting information for: Social modulation of individual preferences in cockroaches

Yannick Günzel, Jaclyn McCollum, Marco Paoli, C. Giovanni Galizia, Inga Petelski and Einat Couzin-Fuchs

Corresponding Author Einat Couzin-Fuchs
E-mail: einat.couzin@uni-konstanz.de

This PDF file includes:

1. Figures: Figs. S1 to S4
2. Transparent Methods

1. Figures

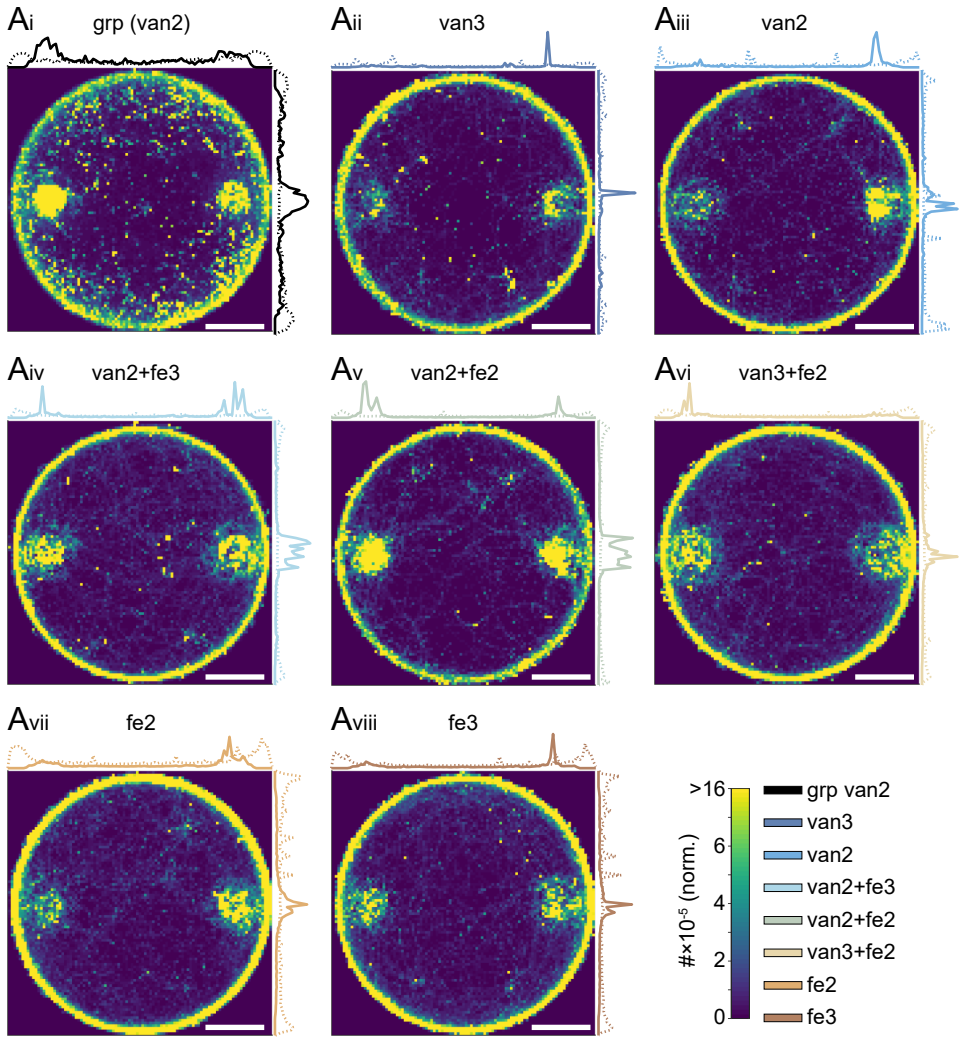

Fig. S1 Density maps for each condition. Extension for Figure 2: Density maps of animal positions over all trials for the group condition (A_i) and single animals ($A_{ii-viii}$). As in Figure 2, coordinate maps were rotated such that the odour shelter is center-right and control is center-left. Heatmaps were normalized to 1 and averaged across animals. Presence densities across and along the arena are indicated above and beside the heat maps, separated for the outer (wall-following bouts, dotted lines) and inner (solid lines) part of the arena. Scale bars: 20 cm. Abbreviations: grp, group; van2(3), vanillin $10^{-2(3)}$; fe2(3), feces extract $10^{-2(3)}$.

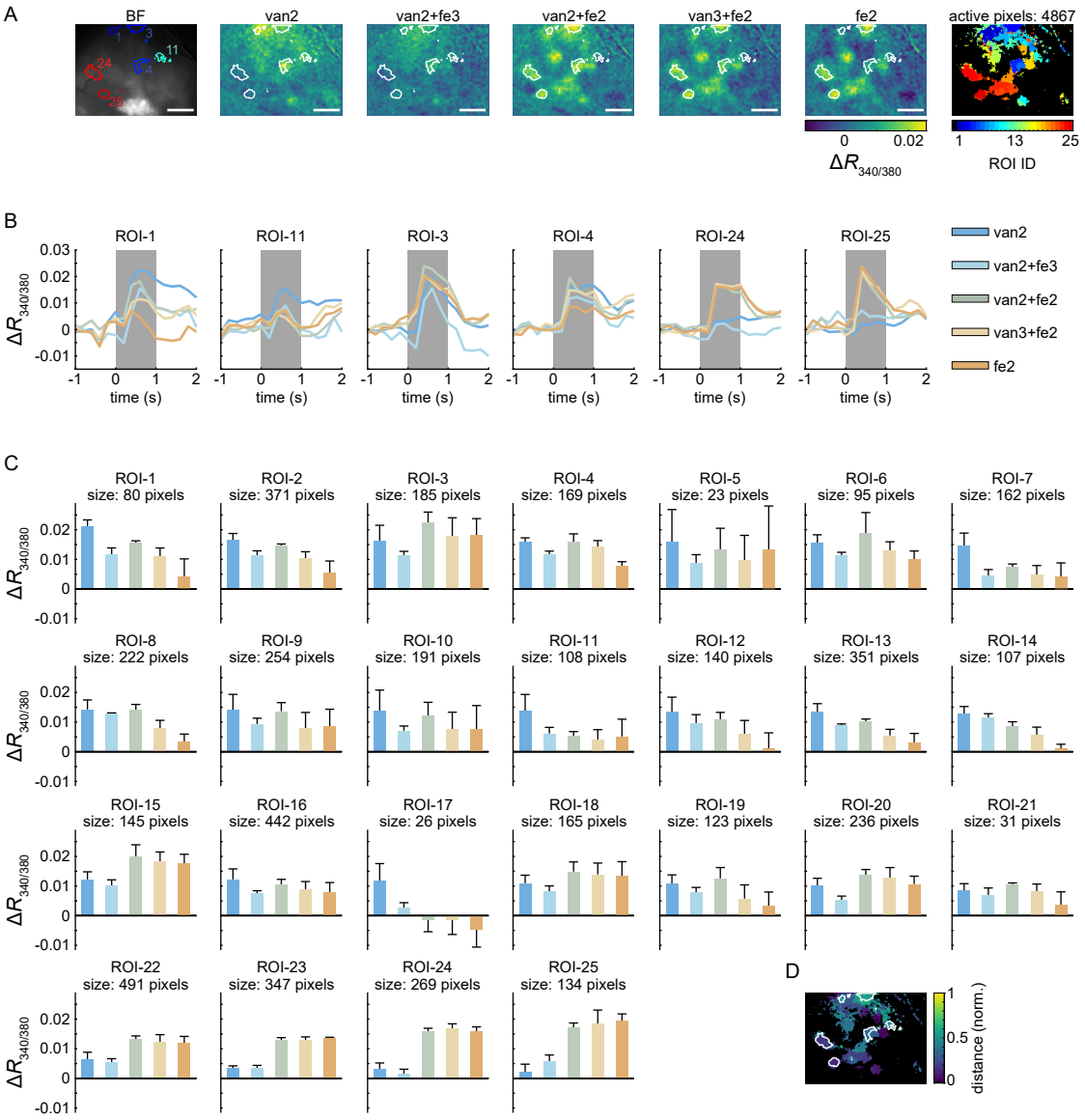

Fig. S2 Spatial and temporal response maps - Example animal mp03, Figure 5Bi. (A) As in figure 5Bi, antennal lobe (AL) bright field microscopy image (greyscale), false colour-coded images of the AL after olfactory stimulation, and distribution of regions of interests (ROIs) resulting from k-medoids clustering on active pixels (>0.01 $\Delta R_{340/380}$ for at least one of the five odours) for two representative individuals. ROI identities were sorted by the corresponding average vanillin-responsiveness (response to van2). Numbers within the bright field image indicate selected exemplary ROIs analysed in the corresponding panels in (B). Each response intensity map is the average response pattern of different repetitions of the same stimulus. Scale bars: 100 μm. (Same as Fig.5Bi) (B) Average temporal responses of six example ROIs to the five different odour stimuli. (C) For all 25 ROIs, the mean response intensity $\pm$ SEM (n = 3-4 repetitions) to the five olfactory stimuli is shown. (D) Medoid variability resulting from different runs. Cluster procedure has been repeated 25 times and for each pixel, the average Euclidean within-pixel distance between the 25 assigned medoids, scaled by the grand mean of between-cluster Euclidean distances, is used as proxi for variability. Abbreviations: van2(3), vanillin $10^{-2(3)}$; fe2(3), feces extract $10^{-2(3)}$.

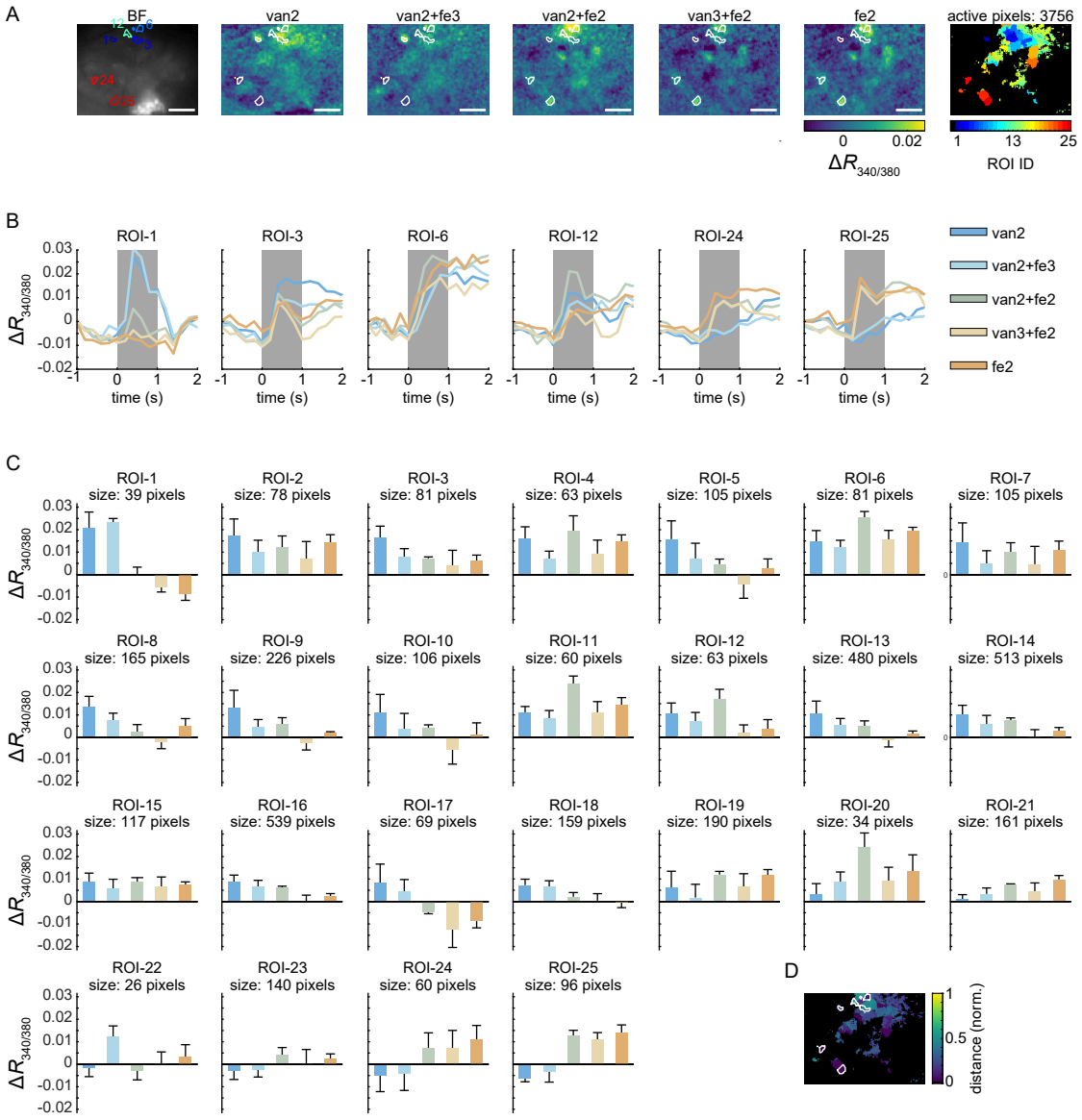

Fig. S3 Spatial and temporal response maps - Example animal mp04, Figure 5Bii. (A) As in Fig.5Bii, antennal lobe bright field microscopy image (greyscale), false colour-coded images of the AL after olfactory stimulation, and distribution of regions of interests (ROIs) resulting from k-medoids clustering on active pixels (>0.01 $\Delta R_{340/380}$ for at least one of the five odours) for two representative individuals. ROI identities were sorted by the corresponding average vanillin-responsiveness (response to van2). Numbers within the bright field image indicate selected exemplary ROIs analysed in the corresponding panels in (B). Each response intensity map is the average response pattern of different repetitions of the same stimulus. Scale bars: 100 μm. (B) Average temporal responses of six example ROIs to the five different odour stimuli. (C) For all 25 ROIs, the mean response intensity ± SEM (n = 3-4 repetitions) to the five olfactory stimuli is shown. (D) Medoid variability resulting from different runs. Cluster procedure has been repeated 25 times and for each pixel, the average Euclidean within-pixel distance between the 25 assigned medoids, scaled by the grand mean of between-cluster Euclidean distances, is used as proxi for variability. Abbreviations: van2(3), vanillin $10^{-2(3)}$; fe2(3), feces extract $10^{-2(3)}$.

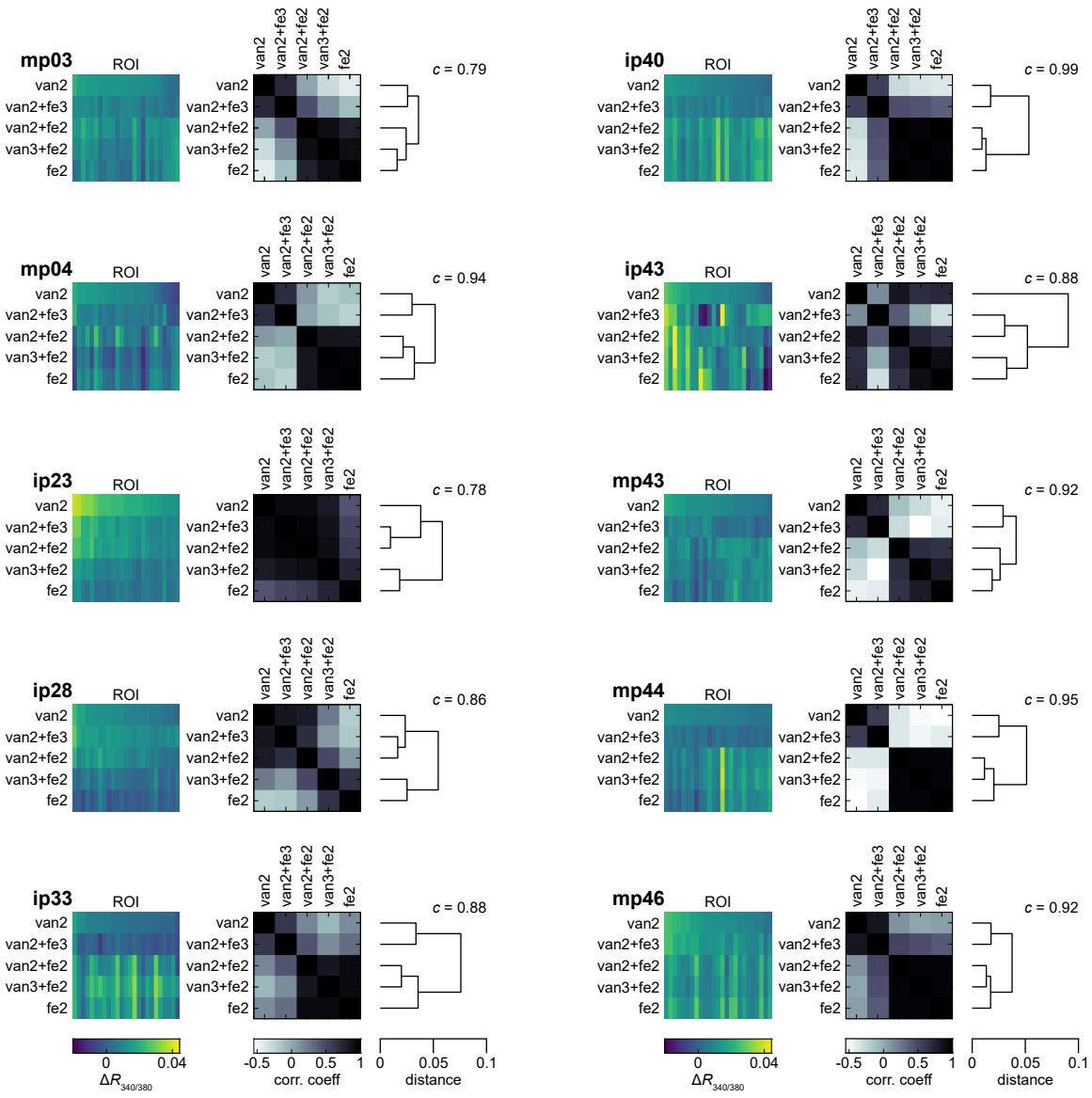

Fig. S4 Analysis of evoked response of ten cockroaches, whose response vectors are shown in Figure 5G. For each animal, response vector maps over all 25 ROIs for the five olfactory stimuli (sorted according to van2 response intensity), together with corresponding Pearson correlation analysis and resulting linkage tree based on agglomerative hierarchical clustering. Cophenetic correlation coefficients c, were used as indication on clustering accuracy. Abbreviations: van2(3), vanillin $10^{-2(3)}$; fe2(3), feces extract $10^{-2(3)}$.

Transparent Methods

Animals. Experiments were performed using adult male *Periplaneta americana* from the animal facility of the University of Konstanz (Germany). Animals were reared under constant conditions and kept on a 12/12 h light/dark cycle with 24 °C and 65 % humidity.

Behavioural experiments. The experimental setup (figure 1A) was inspired by (**?**). Subjects were tested in a circular arena of 90 cm in diameter made of PVC. Petroleum jelly (Balea Vaseline, dm-drogerie markt GmbH + Co. KG, Karlsruhe, Germany) was applied to the arena wall to prevent animals from climbing. A transparent Plexiglas plate covered the top of the arena, while the base contained six small, equally spaced holes, in which odours were inserted and administered from below. Two shelters (diameter: 12 cm; height: 2 cm) covered in a transparent red filter paper (LEE filter film No. 106; Primary Red) were placed above two opposing holes, selected randomly from the different odour outlets to form the odour and control shelters. The arena base and shelters were cleaned after each trial in order to remove any remaining chemical traces. All experiments were recorded at 25 fps with a single Basler camera (acA2040 - 90 μm; Basler AG, Germany) with IR long pass filter, located above the arena. A grid array of IR 850 nm wavelength with a diffuser plate was placed below the arena for uniform light conditions in the video recordings. Additional ceiling light provided an ambient illumination. Temperature was kept between 24 °C and 26 °C during experiments. All trials started five minutes after odour administration and lasted 30 minutes. In total, 105 animals were used for individual trials (15 animals per odour condition) and 201 animals for the 10 group trials (in one case, 21 individuals were used).

Odour preparation. *Periplaneta americana* faeces extract was provided by H. Nishino (Hokkaido University, Japan). Faeces was collected from a colony of cockroaches fed exclusively on agarose, to reduce the presence of secondary metabolites originating from food. Both butter vanillin (Dr. Oetker, Bielefeld, Germany) and the faeces extract were diluted to 10^{-2} and 10^{-3} in 1 mL of mineral oil (CAS 8042-47-5, cat.num. 124020010, Acros Organics, Thermo) in 1.5 mL glass vials for behavioural experiments. For a control, 1 mL of pure mineral oil was placed under the control shelter, opposite to the odour vial in each trial. odours were prepared fresh at the beginning of each day of experiments. For calcium imaging the same dilutions were prepared in 1 mL mineral oil and placed in 20 mL glass vials, covered with nitrogen (Sauerstoffwerk Friedrichshafen GmbH, Friedrichshafen, Germany) and sealed with Teflon septum (Axel Semrau GmbH, Sprockhövel, Germany).

Tracking and data analysis. Behavioural videos were processed in FFmpeg (http://ffmpeg.org/). Tracking of all animals were obtained using a version of the Python-based program Tracktor [Sridhar et al., 2019], modified to better keep individual identities after crossing events. Animals were considered 'sheltered' when their body centroid had stayed for at least 0.5 s within a radius of 7 cm around the shelter's centre. Special care was taken that identities of sheltered animals during group trials were not switched. For this, tracking of each sheltered animal for each video was manually corrected using a custom-written GUI in MATLAB (R2020a, The MathWorks Inc, Natick, MA, USA). Since shelter locations in different trials were randomly selected out of six possible positions, animal trajectories were rotated to set the odour outlet as a single position in all trials. Hence, in all figures, the odour shelter is presented on the right and the control on the left.

Data was analysed and plotted using custom-written MATLAB scripts. Density maps represent 2D histograms (100x100 equally-spaced pixel bins) of animal presence, normalized by duration and number of tested animals. They were generated using the entire data set of one condition. To separate wall-following behaviour, tracked locations were divided into an inner (distance to the centre of the arena smaller than 0.85 times arena radius) and an outer subset, as indicated in figure 2A). In order to get a good estimate for estimator properties, *e.g.* spread of the data, trial averages of behavioural data were re-sampled (B = 10'000 bootstrapped means of random samples).

Shelter/quarter preference indices (figure 2B and figure 3A$_{iv}$ and 3B$_{iv}$) were calculated as the proportion of time spent in the odour shelter/quarter minus the proportion of time in the control shelter/quarter, divided by the sum of both. Similarly, entry index (figure 2C and 4A$_{iii}$), and permanence index (figure 4B$_{iii}$) were calculated based on the proportion of entries and the integral under the permanence probability curves (showing for each time point the probability of staying in a shelter for at least that time) in the odour shelter, minus those in the control shelter, divided by the sum of both. Therefore, for each preference index a value of -1 indicates a complete preference for the control, and a value of +1 a complete preference for the odour.

Behavioural similarities across the different tested conditions were evaluated using agglomerative hierarchical clustering of the data. Similarities were based on the Euclidean distance among conditions each described by four different preference indices (shelter, quarter, entry, survival). Clustering was based on the unweighted average distances between conditions and evaluated by calculating the cophenetic correlation coefficient, which provides an indication on how accurately the clustering reflects the data (values close to one indicating an accurate cluster solution).

Neurophysiology - Calcium imaging. Calcium Imaging was performed in the right antennal lobe of adult male cockroaches, with the dye application method to stain projection neurons following [Paoli et al., 2020], adapted from [Paoli et al., 2017] and [Sachse and Galizia, 2002]. On the first day, animals were anesthetized with CO_2 to facilitate handling. Cockroaches were then placed into a custom-built holder with their heads restrained by soft dental wax. An incision creating a small window was

made in the cuticle of the head to expose the injection site. A crystal of calcium sensitive 10 kDa dextran-conjugated Fura-2 (Thermo Fisher Scientific, Waltham, MA, USA) was injected medio-ventrally into the medial calix of the right mushroom body using a glass capillary. After dye injection, the head capsule was sealed to prevent brain desiccation. The following day, the AL was re-exposed to allow optical access, and the brain was covered in transparent two-component silicon (Kwik-Sil, WPI, Sarasota, FL, USA) for imaging experiments.

Calcium imaging analysis was performed at a widefield fluorescence microscope (BX51WI, Olympus, Tokyo, Japan) equipped with a 10x water immersion objective (Olympus UM Plan FI 10x/0.30w). Images were acquired with a SensiCam CCD camera (PCO AG, Kelheim, Germany) using 120x160 pixel frames and a pixel size of 3.75 μm x 3.75 μm. Recordings were acquired at 5 fps using TILLvisION acquisition system (TILL Photonics, Graefelfing, Germany). A LED system equipped with a 340 and a 385 nm LED (Omicron-Laserage Laserprodukte GmbH, Rodgau-Dudenhofen, Germany) was employed as light source, which was directed onto the cockroach brain via a 410 short-pass filter and a 410 dichroic mirror. Emitted light was filtered through a 440 long-pass filter.

Olfactory stimulation. Olfactory stimulation during calcium imaging analysis was performed with an automatic multi-sampler for gas chromatography (Combi PAL, CTC Analytics AG, Zwingen, Switzerland). Two 1 s odour pulses were injected at 4 s and 12 s with an injection speed of 1 mL/s into a continuous flow of 1 mL/s of purified air. The stimulus was directed towards the right antenna via a Teflon tube (inner diameter, 0.87 mm; length, 40 cm), and the antenna was inserted into the terminal portion of the tube to ensure similar stimulation conditions across animals. Ten cockroaches were tested with 9 different stimuli (van10^{-4}; van10^{-3}; van10^{-2}; van10^{-3}+fe10^{-3}; van10^{-2}+fe10^{-3}; van10^{-2}+fe10^{-2}; van10^{-3}+fe10^{-2}; fe10^{-3}; fe10^{-2}) and with pure mineral oil as control. For each animal, the order of exposure was pseudo-randomized, although keeping the order of increasing concentrations (*i.e.* decreasing dilution) for each pure odorant (*e.g.* van10^{-4}, van10^{-3}, and van10^{-2}). The whole of nine olfactory stimuli was repeated either three or four times (depending on animal responsiveness). An inter-trial interval of two minutes was kept between stimuli, during which the syringe was flushed with clean air. After each set of stimuli, the syringe was washed with *n*-pentane (Merk KgaA, Darmstadt, Germany), heated to 44 °C, and flushed with clean air.

Calcium imaging data analysis. Calcium imaging recordings were exported and processed in MATLAB. We adopted a ratiometric protocol for calcium imaging using Fura-2 excitation wavelengths of 340 and 380 nm. Ratios of 340 to 380 nm signals were calculated ($R_{340/380}$) and the offset was removed by subtracting the mean signal before odour stimulation ($\Delta R_{340/380}$). Response maps for each frame were smoothed with a 4-by-4 window using 2D median filtering. For each repetition, the response to the solvent (mineral oil) was subtracted from all stimulus-induced responses, and the average odour response map was calculated across the 3 (or 4) repetitions of each stimulus conditions. Regions of interest (ROIs) were automatically segmented using *k*-medoids functional clustering on all time traces of all active pixels, *i.e.* regions showing a stimulus-induced increase in fluorescence $\Delta R_{340/380}$ >0.01 for at least one of the five odours. For the cluster analysis, we considered each active pixel as object, whose features were the concatenated responses to each stimulus, resulting in 400 features (five stimuli times 80 frames per stimulus). Dimensionality was then reduced by principal component analysis on the input data set. Thus, to group pixels based on their activity, we only considered the principal components that together explain 95 % of the variance. The initial cluster central positions were determined using a preliminary clustering phase on a random subsample of 10 % of the data. The algorithm ran until a maximum number of 10'000 iterations over 100 replicates. We set the number of clusters - thus the number of ROIs - to $k = 25$, as this reflects the total possible number of response types of five different stimuli ($k = N^s$; for $N = 5$ odour stimuli and $s = 2$ ways of responding, *i.e.* 'response' vs. 'no response'), and provides a good approximation of the number of glomeruli that can be detected on a superficial plane of the cockroach antennal lobe. Other parameters, *e.g.* the distance metric, were kept at their default (standardized Euclidean distance in this example; see MATLAB's kmedoids-function for details). Since medoid-initialisation is based on random processes, we repeated the clustering 20 times and evaluated the resulting variability with the mean within-pixel Eucidean distance between the 20 assigned medoids, scaled by the mean between-ROI Eucidean distance resulting from the 20 runs (figure S3D and S4D). Resulting ROIs were sorted according to their response to vanillin (van10^{-2}). For each individual, stimulus-specific response vectors were obtained as mean responses of each ROI across repetitions. Response similarities were then assessed by calculating the Pearson's correlation coefficients between response vectors of the different odour conditions, which were then used to construct a dendrogram according to an agglomerative hierarchical clustering method (following the same principle as for the behavioural data - see subsection 'Tracking and data analysis' above). For graphical representation, responses' heatmaps (figure 5B and figure S2) present average odour response maps between 0.6 s and 1s after stimulus onset, across repetitions.

Statistical analysis. If not stated otherwise, bar plots with error bars indicate means and standard deviations. Violin plots are used to show the probability density estimate of the bootstrapped data, while values that were either 1.5xIQR above the 0.75 quantile or 1.5xIQR below the 0.25 quantile were excluded from the violins but depicted as points. Horizontal lines within the violins indicate means. We used a bootstrap-based randomization test to evaluate the statistical significance of our data (Eq. 1). For this, we estimated the probability p of observing our sample test statistic $t(x)$ or something even more extreme in the bootstrapped test statistic $t(x^{*b})$, given the null hypothesis is true (for two detailed examples on hypothetical data including calculation paths and resulting implications, see data repository: https://bwsyncandshare.kit.edu/s/JHMzqea7B53Kct6).

$$p = \frac{\#[t(x^{*b}) \geq t(x)]}{B} \quad [1]$$

For a one-sample hypothesis test, estimating whether the mean of the population is statistically significantly different from a pre-determined value μ_0, *e.g.* 0.5, we evaluated the test statistic $t_1(\bullet)$ (Eq. 2) on the observed sample x with sample size n, and on each bootstrap sample x^* of the empirical distribution $\tilde{x}_i = x_i - \bar{x} + \mu_0, i = 1, \ldots, n$.

$$t_1(x) = \frac{|\bar{x} - \mu_0|}{\sigma_x / n} \quad [2]$$

$$t_1(\tilde{x}^{*b}) = \frac{|\bar{\tilde{x}}^* - \mu_0|}{\sigma_{\tilde{x}^*} / n}$$

For a two-sample hypothesis test of comparing the sample z with sample size n, and sample y with sample size m we followed a similar principle. We evaluated the test statistic $t_2(\bullet)$ (Eq. 3) on the observed samples and on each bootstrap sample coming from a combined sample of z and y, denoted as x. Meaning, we randomly drew with replacement and the size of $n + m$ from x and assigned the first n samples to z^* and the remaining m samples to y^*. Then, this has been repeated B times.

$$t_2(z, y) = \frac{|\bar{z} - \bar{y}|}{\sqrt{\sigma_z / n + \sigma_y / m}} \quad [3]$$

$$t_2(\tilde{z}^{*b}, \tilde{y}^{*b}) = \frac{|\bar{\tilde{z}}^* - \bar{\tilde{y}}^*|}{\sqrt{\sigma_{\tilde{z}^*} / n + \sigma_{\tilde{y}^*} / m}}$$

Note, with the absolute difference in the numerators of Eq. 2 and Eq. 3, respectively, our test statistics yield a two-tailed comparison.